Galaxy Zoo Builder: Morphological Dependence of Spiral Galaxy pitch angle

Timothy Lingard[1]⋆, Karen L. Masters[2], Coleman Krawczyk[1], Robert C. Nichol,[1]

[1] *Institute of Cosmology and Gravitation, University of Portsmouth, Dennis Sciama Building, Burnaby Road, Portsmouth, PO1 3FX, UK*
[2] *Haverford College, 370 Lancaster Ave., Haverford, PA 19041, USA*

ABSTRACT
Abstract

Key words: galaxies: evolution – galaxies: spiral – galaxies: photometry

1 INTRODUCTION

Spiral structure is present in a majority of massive galaxies (Buta 1989, Lintott et al. 2008) yet the formation mechanisms through which spiral structure originates are still hotly debated. Spirals are as diverse as the theories proposed to govern their evolution; from the quintessential pair of well-defined arcs of the grand design spiral, to the fragmented arm segments of the flocculent spiral, to the disjointed multi-armed spiral. These variatons on structure account for 18%, 50% and 32% of the population respectively (Elmegreen et al. 2011, Buta et al. 2015).

Arms of spiral galaxies are the source of the vast majority of star formation in the Universe, and spirals rearrange disc gas and can lead to the formation of disc-like bulges (e.g. Kormendy & Kennicutt 2004). Studies of spiral morphology have found interesting correlations between spiral morphology and other galactic properties, such as a correlation between spiral tightness and central mass concentration (Yu & Ho 2019, Davis 2015, though Hart et al. 2017 found no such relation) and tightness and rotation curve shape (Seigar et al. 2005, with rising rotation curves creating more open spiral structure). These predictions and observations provide compelling reasons for investigating their underlying rules and dynamics, as doing so is essential for understanding the secular evolution of disc galaxies.

1.1 Formation and Evolution of Spiral Arms

Our current understanding of the mechanisms which drive spiral growth and evolution suggest that each of the different forms of spiral galaxy may be triggered primarily by different processes. Grand Design spirals are thought to have undergone a tidal interaction, be driven by a bar (as seen in gas simulations, Sanders & Huntley 1976, Rodriguez-Fernandez

& Combes 2008, and suggested for stars by Manifold theory, Romero-Gómez et al. 2006, Athanassoula et al. 2009a, Athanassoula et al. 2009b), or be obeying (quasi-stationary) density wave theory (QSDW theory), in which spiral arms are slowly evolving, ever-present structures in the disc (Lin & Shu 1964). Flocculent spirals are thought to be formed through swing amplification (shearing of small gravitational instabilities in the disc), and be transient and reccurent in nature (Julian & Toomre 1966). It is recognised that methods of spiral formation are not mutually exclusive.

One of the fundamental assumptions of early work on spiral formation mechanisms (primarily QSDW) was that the disc of a galaxy, if unstable to spiral perturbations, would create a stable, static wave which would exist unchanging for many rotational periods (Lin & Shu 1964). The motivation for static waves with small numbers of arms (with a preference for $m = 2$) was primarily observational; most galaxies show spiral structure, indicating that spirals exist for a long time or are continually rebuilt.

Many simulations demonstrate that spirals do not maintain a constant pitch angle, and instead wind-up over time due to the differential rotation of the disc (Baba et al. 2013). Recent research suggests that spirals are dynamical in nature, and continually dissapate and re-form (Dobbs & Baba 2014). These spirals can be maintained through the same mechanisms that drive QSDW spirals (i.e. WASER, Mark 1976, swing amplification, Goldreich & Lynden-Bell 1965), but do not require the idealistic disc conditions required for the formation and maintenance of a stationary wave. The pitch angles of these transient spiral arms will decrease due to the differential rotation of the disk, with the density of the arm peaking at some critical pitch angle and then dissapating to be reformed.

In this dynamic picture of spiral arms, pitch angle monotonically decreases from a spiral arm's formation to its dissapation. Pringle & Dobbs (2019) proposes a simple test of spiral arm winding, assuming the cotangent of the pitch angle evolves linearly with time. Finding compelling evid-

---

⋆ E-mail: tim.lingard@port.ac.uk

ence of this relationship against QSDW theory, in favour of the dynamic spirals now favoured by many simulations.

Spiral evolution also appears to be influenced by the presence and strength of a bar; in barred grand-design spirals the arms often appear to start from the ends of the bar. Simulations of gas in barred galaxies often demonstrate that bars can drive long-term spiral evolution (Rodriguez-Fernandez & Combes 2008), or boost transient spiral structure (Grand et al. 2012). Manifold theory is one attempt to determine the orbits of stars in bar-driven spiral arms: it proposes that stars in the vicinity of the unstable Lagrangian points at either end of the bar tend to escape along predictable orbits, governed by invariant manifolds. One of the primary factors influencing the shape of this invariant manifold is the relative strength of the non-axisymmetric forcing caused by the bar, with stronger bars resulting in spirals with larger pitch angles.

Many other systems contribute to spiral morphology, including potential ties to bulge fraction (Yoshizawa & Wakamatsu 1975, Savchenko & Reshetnikov 2013, Masters et al. 2019) and black hole mass (Davis 2015, Davis et al. 2017), via a series of correlations. Stronger bulges and more more massive central black holes are both linked to more tightly wound spiral arms, albeit with large amounts of scatter.

1.2 Measuring galaxy pitch angle

Many methodologies have been proposed and implemented to measure spiral arm properties, including visual inspection (Herrera-Endoqui et al. 2015), fourier analysis (i.e. 2DFFT, Davis et al. 2012), texture analysis (i.e. SpArcFiRe, Davis & Hayes 2014), and combinations of automated methods and human classifiers (Hart et al. 2017, Hewitt & Treuthardt 2020). One potentially underused method of obtaining measurements of spirals is through photometric fitting of spiral structure, as possible using tools such as GALFIT (Peng et al. 2010) and *Galaxy Builder* ([[**Lingard et al. (2020)**]]). These methods attempt to localize light from an image of a galaxy into distinct subcomponents, such as a galaxy disc, bulge, bar and spiral arms, generally finding the optimum solution using computational optimization. This optimization process, however, is often not robust for complex, many-component models and requires significant supervision to converge to a physically meaningful result (Gao & Ho 2017). [[**Lingard et al. (2020)**]]propose a solution to this problem through the use of citizen science to provide priors on parameters used in computational fitting.

A common assumption when measuring galaxy pitch angle is that observed spiral arms have a constant pitch angle. Spirals of this kind are known as logarithmic spirals and are described by

$$r = A \, e^{\theta \tan \phi},$$ (1)

where ϕ is the arm's pitch angle. One method used to obtain a pitch angle of a galaxy is to fit logarithmic spirals to individually identified arm segments and take the weighted mean of their pitch angles (which often vary by upwards of $10°$, Davis & Hayes 2014). Weighting is determined by the length of the arc segment, with longer being assigned higher

weights, i.e. for a galaxy where we have identified N arm segments, each with length L_i and pitch angle ϕ_i

$$\phi_{\mathrm{gal}} = \left(\sum_{i=1}^{N} L_i \right)^{-1} \sum_{i=1}^{N} L_i \phi_i.$$ (2)

The most commonly used measurement of uncertainty of length-weighted pitch angles is the unweighted sample variance between the arm segments identified.

A notable drawback of length-weighted pitch angle is sensitivity to the number and quality of the spiral arm segments identified; Hart et al. (2017) found that only 15% of the arm segments identified by a leading algorithm (SpArcFiRe) were identified as "good" matches to real spiral arms by citizen science classifiers.

Fourier analysis in one- and two-dimensions (as performed by Díaz-García et al. 2019, Davis et al. 2012, Mutlu-Pakdil et al. 2018) is another widely used method of computationally obtaining galaxy pitch angles. Two-dimensional fourier methods generally decompose a deprojected image of a galaxy into a superpositions of logarithmic spirals between inner and outer annuli (Davis et al. 2012), and reports the pitch angle with the highest amplitude as the galaxy's pitch angle. Hewitt & Treuthardt (2020) combined fourier analysis of spiral galaxies with human tracing of spiral arms, to great effect. It is uncertain how variation between pitch angles of individual arms impacts this measurement.

This paper makes use of the classification data and fitted photometric models obtained through the *Galaxy Builder* citizen science project for the 196 spiral galaxies present in [[**Lingard et al. (2020)**]]. In this paper we focus on the use of measured spiral tightness (quantified using pitch angle, Binney & Tremaine 1987) as a probe into the dynamical mechanisms governing a spiral galaxy's evolution. We make use of Bayesian hierarchical modelling to measure galaxy pitch angle from the spiral arm clusters produced by *Galaxy Builder*.

Section 3.2 investigates spiral arm winding using the test derived by Pringle & Dobbs (2019) (uniformity of galaxy pitch angle in cot ϕ) and concludes using a marginalized Anderson-Darling test that we cannot unilaterally reject winding of this form at the 1% level. Section 3.3 examines the correlation between pitch angle and bulge size implied by the Hubble sequence, and pitch angle and bar strength implied by Manifold theory, and find no significant correlation.

2 METHOD

2.1 The Galaxy Sample

The galaxies analysed in this paper are the 198 galaxies from [[**Lingard et al. (2020)**]]. These are a subset of the *stellar mass-complete sample* in Hart et al. (2017), a sample of low-redshift face-on spiral galaxies selected using data from the NASA-Sloan Atlas (Blanton et al. 2011) and Galaxy Zoo 2 (Willett et al. 2013).

Some galaxies in [[**Lingard et al. (2020)**]]were shown to volunteers again in a repeat *validation subset* in order to create a second aggregate model used to test internal consistency. We combine the classifications of galaxies in this

validation subset with the original classifications. Clustering of drawn spiral arms and cleaning of points was then performed as detailed in [[**Lingard et al. (2020)**]]. We remove any galaxies for which fewer than two spiral arms were identified [[**why exclude one-armed?**]]. This results in a hierarchical data structure of 91 galaxies, 211 spiral arms and 215,678 points.

Spiral arm points are deprojected to a face-on orientation using the disk inclination and position angle obtained through photometric model fitting performed in [[**Lingard et al. (2020)**]].

2.2 Bayesian modelling of spiral arms in *Galaxy Builder*

We model a spiral arm as a logarithmic spiral, described by

$$r_{\mathrm{arm}} \sim \mathcal{N}\left(\exp\left[\theta_{\mathrm{arm}} \tan\phi_{\mathrm{arm}} + c_{\mathrm{arm}}\right], \sigma_r\right). \qquad (3)$$

Assume the pitch angle of a galaxy's spiral arms are drawn from a Normal distribution, truncated between 0 and 90 degrees, centred on some value we will call the galaxy's pitch angle, ϕ_{gal}. This dispersion in arm pitch angle has some measure of spread, σ_{gal}, which we will assume is the same in all galaxies:

$$\phi_{\mathrm{arm}} \sim \mathrm{TruncatedNormal}(\phi_{\mathrm{gal}}, \sigma_{\mathrm{gal}}, \min = 0, \max = 90). \qquad (4)$$

We choose hyperpriors on ϕ_{gal} and σ_{gal} of

$$\phi_{\mathrm{gal}} \sim \mathrm{Uniform}(\min = 0, \max = 90), \qquad (5)$$

$$\sigma_{\mathrm{gal}} \sim \mathrm{InverseGamma}(\alpha = 2,\ \beta = 20). \qquad (6)$$

We also have the offset parameter c, and a measure of radial uncertainty σ_r:

$$c_{\mathrm{arm}} \sim \mathrm{Cauchy}(\alpha = 0,\ \beta = 10), \qquad (7)$$

$$\sigma_r \sim \mathrm{HalfCauchy}(\beta = 0.2). \qquad (8)$$

Our likelihood function is therefore

$$\mathcal{L} \sim \mathcal{N}\left(\exp\left[\theta_{\mathrm{arm}} \tan\phi_{\mathrm{arm}} + c_{\mathrm{arm}}\right], \sigma_r\right). \qquad (9)$$

To perform inference, we make use of the No-U-Turn-Sampler (NUTS, Hoffman & Gelman 2011), implemented in PYMC3[1], an open source probabilistic programming framework written in python (Salvatier et al. 2016). We scale the radii of deprojected points to have unit variance, to aid the convergence of MC chains.

3 RESULTS

3.1 Constraints on Galaxy Pitch angle

Our hierarchical model identifies arm pitch angle with a high degree of certainty (uncertainty less than 1.6°for 95% of arms, assuming no error on disc inclination and position

---

[1] https://docs.pymc.io/

angle), however it returns a large spread of potential values for the pitch angles of galaxies, primarily caused by only measuring pitch angles of a small number of arms per galaxy. For galaxies with two arms identified in *Galaxy Builder*, we have a mean uncertainty of 7.8°, which decreases to 6.7°and 5.8°for galaxies with three and four arms respectively.

Our measure of inter-arm variability of pitch angle, σ_{gal} has a posterior distribution of 11.02 ± 0.95, confirming the finding of Davis & Hayes (2014) and emphasising the need for fitting algorithms to not assume all arms have the same pitch angle.

3.2 Spiral Winding

In order to test the possible progenitor distribution of our estimated galaxy pitch angles, we repeatedly perform an Anderson-Darling test over each draw present in the MCMC trace, resulting in a distribution of Anderson-Darling statistics. We will refer to this test as the *marginalized Anderson-Darling test*. We make use of the Kolmogorov-Smirnov test in a similar manner for comparison.

We perform the marginalized Anderson-Darling test for a potential source distribution uniform in $\cot\phi$ between the limits present in Pringle & Dobbs (2019) ($1.00 < \cot\phi < 4.75$, or roughly $11.9° < \phi < 45.0°$). The resulting distribution of Anderson-Darling statistics can be seen in Figure 1. We observe that we reject the null hypothesis at the 1% level for 69% of the possible realizations of galaxy pitch angle. While, with our sample and methodology, we cannot unilaterally reject winding of the kind described by Pringle & Dobbs (2019), it suggests this model is not found in our data.

Not seeing uniformity in $\cot\phi$ is not evidence against spiral winding, nor is it evidence for static spiral structures. Our results simply suggest that a more comprehensive test is needed for observational data of this kind.

3.3 Dependence of pitch angle on Galaxy Morphology

#### 3.3.1 Pitch angle vs. Bulge size

We see no correlation between galaxy pitch angle derived from the hierarchical model and Galaxy Zoo 2's debiased (Willett et al. 2013) *pbulge*, which has been shown to be a good measure of bulge size.

We separate our sample into "disc-dominated galaxies" and "obvious bulge galaxies" using the debiased fractions from Galaxy Zoo 2 following Kruk et al. (2017), defining *no bulge + just noticeable > obvious + dominant* for the former and the converse for the latter. A marginalized two-sample Anderson-Darling test (Scholz & Stephens 1987) does not find any evidence that the samples were drawn from different distributions; we do not reject the null hypothesis at the 1% level for any samples. The distribution of Anderson-Darling test statistics is shown in the upper panel of Figure 2.

3.3.2 Pitch angle vs. Bar Strength

We see no correlation between galaxy pitch angle derived from the *hierarchical normal model* and Galaxy Zoo 2's debiased *pbar*, which is widely viewed as a good measure
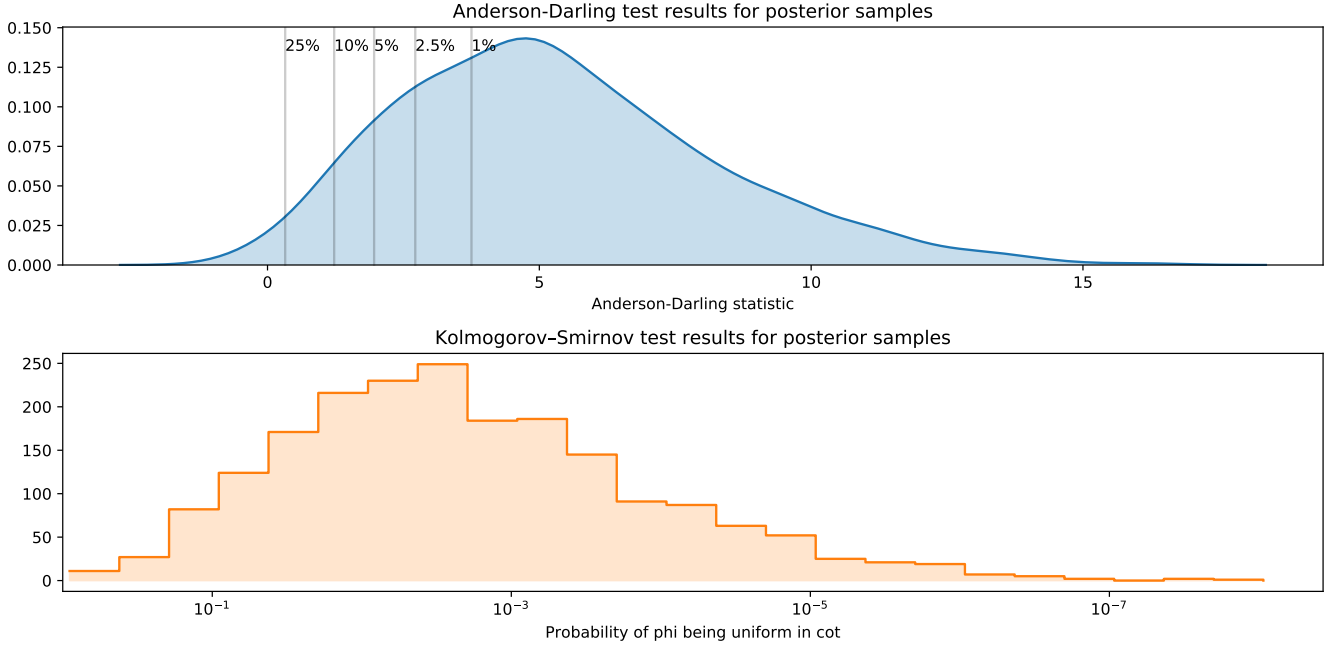
Figure 1. The results of a marginalized Anderson-Darling test (top panel), with values corresponding to various confidence intervals shown, and marginalized Kolmogorov-Smirnov test p-values (lower panel). Moving rightwards on the x-axis implies greater confidence in rejecting the null hypothesis.

of bar strength, and therefore a measure of the torque applied on the disc gas.

Separating the sample based off of *pbar* > 0.5, and restricting to galaxies with more than 10 classifications for *pbar* (as performed by Masters et al. 2011 and Kruk et al. 2017) and performing a marginalized two-sample Anderson-Darling test does not find that the samples were drawn from different distributions (we reject the null hypothesis at the 1% level for only 1% of samples). The distribution of Anderson-Darling test statistics is shown in the lower panel of Figure 2.

We do not account for variation in bulge size in this work, however predictions from Manifold theory should not be affected as bulges do not provide a non-axisymmetric focing.

4   DISCUSSION

This paper presents a new Bayesian approach to estimate galaxy pitch angle, making use of citizen science results to measure spiral arms through photometric modelling. We introduce an adaptation of the Anderson-Darling test to incorporate full Bayesian posterior probabilities and utilize this test to investigate theories governing spiral formation and evolution.

The statistical approach implemented in this paper allows a more thorough examination of pitch angle than simpler methods of logarithmic spiral fitting, and better accounts for inter-arm pitch angle variation than fourier analysis, which assumes all arms in a given mode have the same pitch angle.

Our method and results do not completely reject spiral

winding of the form described by Pringle & Dobbs (2019), however this result is highly sensitive to the boundaries used; using limits of $10.0° < \phi < 40.0°$ results in us rejecting the null hypothesis at the 1% level for 99% of the MCMC draws. As no physical justification was provided for the limits present in Pringle & Dobbs (2019), this is a far from ideal test of arm winding.

We do not find a relationship between bar strength and pitch angle, as would have been predicted by Manifold theory, and do not find evidence for the relationship between central mass concentration and pitch angle predicted by the Hubble sequence.

As with most analyses, the most impactful improvement it would be possible to make here would be to increase the cleanliness and volume of data analysed; due to time constraints the *Galaxy Builder* galaxies used are not guaranteed to be representative. However, we believe that the methodlogy proposed here is a scalable, robust solution to the problems facing investigation of spiral morphology.
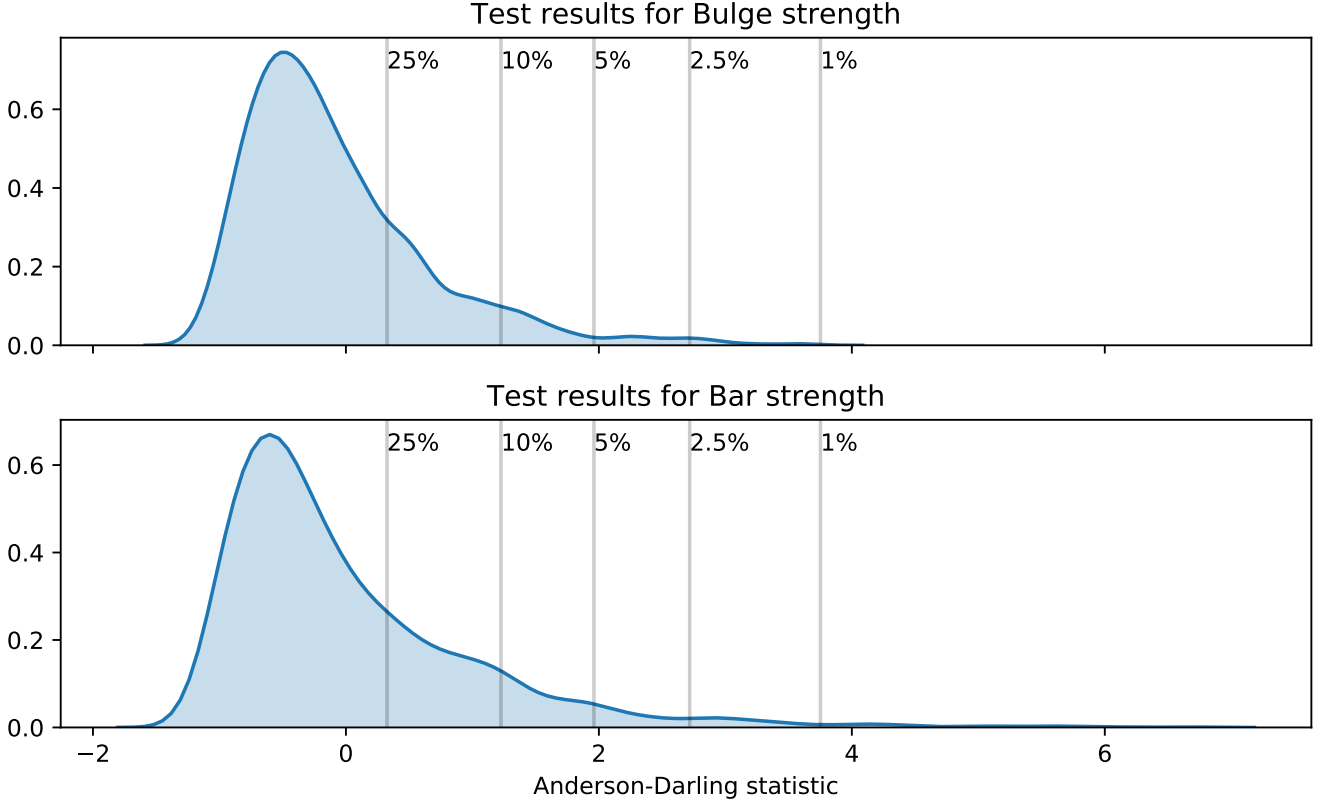
Figure 2. The results of marginalized two-sample Anderson-Darling tests examining whether pitch angles for Bulge-dominated and Disc-dominated galaxies are drawn from the same distribution (top panel), and the results of the same test for strongly-barred vs unbarred galaxies (bottom panel).

References

Athanassoula E., Romero-Gómez M., Masdemont J. J., 2009a, MNRAS, 394, 67
Athanassoula E., Romero-Gómez M., Bosma A., Masdemont J. J., 2009b, MNRAS, 400, 1706
Baba J., Saitoh T. R., Wada K., 2013, ApJ, 763, 46
Binney J., Tremaine S., 1987, Galactic dynamics
Blanton M. R., Kazin E., Muna D., Weaver B. A., Price-Whelan A., 2011, AJ, 142, 31
Buta R., 1989, Galaxy Morphology. p. 151
Buta R. J., et al., 2015, VizieR Online Data Catalog, p. J/ApJS/217/32
Davis B., 2015, PhD thesis, University of Arkansas
Davis D. R., Hayes W. B., 2014, ApJ, 790, 87
Davis B. L., Berrier J. C., Shields D. W., Kennefick J., Kennefick D., Seigar M. S., Lacy C. H. S., Puerari I., 2012, ApJS, 199, 33
Davis B. L., Graham A. W., Seigar M. S., 2017, MNRAS, 471, 2187
Díaz-García S., Salo H., Knapen J. H., Herrera-Endoqui M., 2019, arXiv e-prints, p. arXiv:1908.04246

Dobbs C., Baba J., 2014, Publ. Astron. Soc. Australia, 31, e035
Elmegreen D. M., et al., 2011, ApJ, 737, 32
Gao H., Ho L. C., 2017, ApJ, 845, 114
Goldreich P., Lynden-Bell D., 1965, MNRAS, 130, 125
Grand R. J. J., Kawata D., Cropper M., 2012, MNRAS, 426, 167
Hart R. E., et al., 2017, MNRAS, 472, 2263
Herrera-Endoqui M., Díaz-García S., Laurikainen E., Salo H., 2015, A&A, 582, A86
Hewitt I. B., Treuthardt P., 2020, MNRAS, 493, 3854
Hoffman M. D., Gelman A., 2011, arXiv e-prints, p. arXiv:1111.4246
Julian W. H., Toomre A., 1966, ApJ, 146, 810
Kormendy J., Kennicutt Robert C. J., 2004, ARA&A, 42, 603
Kruk S. J., et al., 2017, MNRAS, 469, 3363
Lin C. C., Shu F. H., 1964, ApJ, 140, 646
Lintott C. J., et al., 2008, MNRAS, 389, 1179
Mark J. W. K., 1976, ApJ, 205, 363
Masters K. L., et al., 2011, MNRAS, 411, 2026
Masters K. L., et al., 2019, MNRAS, 487, 1808
Mutlu-Pakdil B., Seigar M. S., Hewitt I. B., Treuthardt P., Berrier J. C., Koval L. E., 2018, MNRAS, 474, 2594
Peng C. Y., Ho L. C., Impey C. D., Rix H.-W., 2010, AJ, 139, 2097
Pringle J. E., Dobbs C. L., 2019, arXiv e-prints, p. arXiv:1909.10291
Rodriguez-Fernandez N. J., Combes F., 2008, A&A, 489, 115
Romero-Gómez M., Masdemont J. J., Athanassoula E., García-Gómez C., 2006, A&A, 453, 39
Salvatier J., Wiecki T. V., Fonnesbeck C., 2016, PeerJ Computer Science, 55

Sanders R. H., Huntley J. M., 1976, ApJ, 209, 53

Savchenko S. S., Reshetnikov V. P., 2013, MNRAS, 436, 1074

Scholz F. W., Stephens M. A., 1987, Journal of the American Statistical Association, 82, 918

Seigar M. S., Block D. L., Puerari I., Chorney N. E., James P. A., 2005, MNRAS, 359, 1065

Willett K. W., et al., 2013

Yoshizawa M., Wakamatsu K., 1975, A&A, 44, 363

Yu S.-Y., Ho L. C., 2019, ApJ, 871, 194

Appendix

This paper has been typeset from a T_EX/L^AT_EX file prepared by the author.